DOI: 10.71762/7mt5-v498

Research Paper

Comparison of the Microstructure and Mechanical Behavior of the Welding Zone of Aluminum Alloy 5754 by FSW and TIG Methods

Esmaeil Zarei[1] Ahmad Afsari[*1], Eshagh Saharkhiz[2], Seyed Kambiz Ghaemi Osgouie[3]
[1]Department of Mechanical Engineering, Shiraz Branch, Islamic Azad University, Shiraz, Iran
[2]University of Tehran, Kish International Campus, Kish Island, Iran
[3]College of Engineering, University of Tehran, Iran
[*]Email of the Corresponding Authors: Ah.Afsari1338@iau.ac.ir
Received: August 8, 2024; Accepted: September 16, 2024

Abstract
In this research, the weld zones resulting from friction stir welding (FSW) and arc welding with shielding gas and non-consumable tungsten electrodes (TIG) on AL-5754 alloy were compared. The input parameters for both processes were selected based on the Taguchi method, and the welding operations were performed accordingly. To achieve optimal input parameters, tensile, ultrasonic, and hardness tests were conducted on the samples. The results indicated that the weld created by the TIG method exhibited higher tensile strength for samples 3, 4, and 9, with values of 195, 152, and 151 MPa, respectively. However, in FSW, the finer granularity of the base material (44 microns) resulted in a better microstructure (30 microns) compared to the TIG method. This characteristic leads to enhanced mechanical properties, such as toughness, fatigue strength, and flexibility, in the FSW method. Since the hard work done on the base metal is lost with this method, and there is no possibility of increasing the strength of the weld, as can be done with the TIG method by changing the filler material, the TIG method is preferred in this comparison.

Keywords
Al Alloy 5754, Friction Stir Welding, TIG, Microstructure, Mechanical Properties

1. Introduction

Solid state welding is a group of welding processes that produces coalescence at temperatures essentially below the melting point of the base materials being joined, so oxidation does not occur, and no need for shielding gas, neutral environment, and filler metal. Pressure may or may not be used. These processes are sometimes erroneously called solid-state bonding processes. This group of welding processes includes friction, hot pressure, cold, diffusion, ultrasonic, forge, roll, and explosion welding. In all of these processes pressure, time, and temperature individually or in combination produce coalescence of the base metal without significant melting of the base metals. Some of the processes offer certain advantages since the base metal does not melt and form a nugget. The metals being joined retain their original properties without or very small heat-affected zone (HAZ), which is the source of many defects and is one of the main reasons for the reduction of mechanical properties [1].

The friction stir technique played a vigorous role in recent industries as it has been utilized in the welding and processing of metallic materials. Friction stir welding (FSW) is applied for joining poorly weldable materials and enhancing the microstructure and the mechanical properties of the welded joints. Underwater friction stir welding, friction stir spot welding, and vertical compensation friction stir welding are variants of the FSW process. Also, friction stir processing (FSP) is another method, whose basic principal is created from the friction stirring technique, which can be used for manipulating the base materials by performing dynamic recrystallization on grains resulting in superior properties of the processed material. On the other hand, friction stir alloying (FSA) is analogous to FSP with implanted strengthening particles, producing surface composites. Like other fusion welding techniques, the FSW process has its defects which especially characterize the FSW joints. Lack of penetration, voids, tunnels, flash, and surface grooving are the common defects of the FSW method [2].

In general, friction welding is divided into three main groups, including non-rotary friction welding, rotational friction welding, and friction stir welding. In friction welding, mechanical energy is converted into plastic deformation and heat generation [3]. The use of the FSW process in terms of the most used materials in the aerospace industry, there has been the development of new high strength-to-weight ratios such as the 3rd generation aluminum–lithium alloys that have become successfully weldable by FSW with fewer welding defects and a significant improvement in the weld quality and geometric accuracy [4].

On the other hand, dissimilar alloy welding has its techniques that affect the welding quality [5 & 25]. In this regard, studies have been conducted on aluminum alloy 5754 to obtain the superlative possible parameters for welding this alloy by FSW. Also, the hardness of the weld zone has been obtained with a slight increase compared to the base metal to the value of 82 Vickers [6]. In another research, the TIG welding method and the effect of welding defects on the microstructure and strength of aluminum of Al-5754 have been investigated [7]. In this regard, parameters such as argon as a shielding gas with a purity of 99.996%, filling metal made of Al Mg5, current intensity equal to 140 amperes, shielding gas flow rate of 20 liters per minute, with a speed of 0.03 m per minute, has resulted as the best parameters for welding aluminum 5754. Also, the effect of material position on the welding properties created by the FSW method for two dissimilar alloys, aluminum 5052-H32 and 6061-T6, has been studied and compared, and confirmed with the previous results obtained from optical microscopic analysis [8].

During research conducted on Al-4.5Mg-0.26Sc alloy welding (5000 group alloys) using A-TIG and FSW methods, optimal input parameters were obtained. In addition, numerous tests have been performed on the welding of AA5052H32 alloy by TIG and FSW methods, the results indicate that in the optimal condition of the input parameters, the final strength value for TIG mode is 186.5 and for the FSW mode, 202.4 MPa has been obtained. This alloy is widely used in various industries, including automobile manufacturing [9 & 10]. Also, the improvement of mechanical and microstructural properties of AA 5052-H32 alloy in TIG welding using FSP has been investigated [11]. The yield strength of TIG welding joints before processing is 79.5 MPa, but after FSP, it has been upgraded to 129.5 MPa. The tensile strength of TIG welded joints was equal to 176.5 MPa. However, after FSP, it increased to 201 MPa and the results show that FSP has better mechanical properties than untreated TIG welded joints. In this regard, the tests performed on one of the

aluminum alloys show the fact that the final strength and hardness of the part after welding in the FSW method is higher than the value obtained in the TIG method [12].

During research conducted on aluminum alloy AA-5083H321 by FSW and TIG methods with specific input parameters, the ultimate strength of 270 and 231 MPa was obtained for FSW and TIG welding methods, respectively. Also, in this research, Vickers hardness of 99 and 87 was obtained for FSW and TIG, respectively. It should be noted that in this research, the impact test was also performed, and the value of J19 for FSW and J17 for TIG welding was recorded [13]. Comprehensive and Technical investigation of FSW for joining the metal-to-polymer hybrid structures has been done and results indicate that factors such as materials, tools, and process parameters have had a significant influence on the welding method, and in many cases, defects and imperfections have occurred that have a significant effect on the strength and microstructure of the weld [14].

A study has been carried out on 5052-O steel and a comparison of TIG welding and FSW in the best conditions indicates that the final tensile strength values are 140 MPa, the percentage increase in length is 1.7 and the hardness is 32-35 Vickers for The TIG method is obtained. Also, values of 170 MPa, length increase of 7.4%, and hardness of 47-49 Vickers have been recorded for welding by the FSW method. In this regard, a comprehensive review has been conducted regarding the progress of recent research in FSW to create joints of dissimilar materials of aluminum and copper [15]. In research, some of the issues related to FSW of aluminum to copper, such as process parameters, microstructural characteristics, mechanical properties, and electrical characteristics of aluminum and copper joints produced by FSW, have been discussed, and generally, this research aims to increase the joint properties of Al-Cu [16].

Also, a new method to increase the mechanical properties of the Al-5052 alloy joint, which is welded by the TIG method, was invented by Abbasi et al. [17] and the results show that the friction stirs vibration processing is a suitable alternative to the FSP and it has improved the mechanical properties. Also, during a study to achieve an economically suitable welding method and to optimize welding parameters in 5XXX series aluminum with TIG, MIG, and FSW welding methods, it was determined that the hardness of the welded joints compared to the base material AA5083-H111 24-29, 31-35 and 46-50% increase respectively for MIG, TIG and FSW joints. In short, it can be said that reducing the temperature created in the tool and the residual stresses of the workpiece depends on choosing the appropriate speeds for the tool [18, 19].

During recent research, many comparisons have been made between FSW and shielded gas arc welding (TIG). However, no research has been done on comparing FSW and TIG in alloys of Al-5754. Welding parameters and machine parameters will affect the quality of the welded area. In FSW, rotation speed and advance speed are the most important influencing parameters. The group 5000 alloys, which are aluminum-magnesium alloys, have a set of properties of high strength, corrosion resistance, good formability, and weldability by the TIG method, and the mechanical strength and microstructure of this group after welding have been reported to be suitable. To discover the differences, disadvantages, and advantages of each method, some field tests, calculations, and related experiments should be done to know which of the welding methods is suitable for joining aluminum alloys 5754.

2. Materials and Methods

In this research, TIG welding was performed on aluminum alloy 5754 parts. The dimensions of the samples are equal to 120 × 100 × 5 mm. In this process, the welding samples were prepared in the form of a butt joint and its edges were chamfered at an angle of 20 degrees. Before welding, the samples were cleaned with acetone to be free from any type of contamination. The gap between the parts was considered to be 1 mm and they were welded to each other according to Figure 1. The mechanical characteristics of the tested aluminum alloy according to the EN 485-2:2016 (E) standard are presented in Table 1. In this research, TIG welding was performed on aluminum alloy 5754 parts. The dimensions of the samples are equal to 120 × 100 × 5 mm. In this process, the welding samples were prepared in the form of a butt joint and its edges were chamfered at an angle of 20 degrees. Before welding, the samples were cleaned with acetone to be free from any type of contamination. The gap between the parts was considered to be 1 mm and they were welded to each other according to Figure 1. The mechanical characteristics of the tested aluminum alloy according to the EN 485-2:2016 (E) standard are presented in Table 1.

Input parameters for TIG welding are Argon flow (liters per minute), Current density, and welding speed and are selected based on the Taguchi algorithm (Table 3) and each input parameter has three levels. The other three parameters including voltage, electrode diameter, and tungsten electrode type are all fixed and their values are 20V, 2.4 mm, and WT20 respectively [7, 10, 20, and 21]. Based on Taguchi's algorithm, 9 samples were prepared for welding operation, which is presented in Table 4.

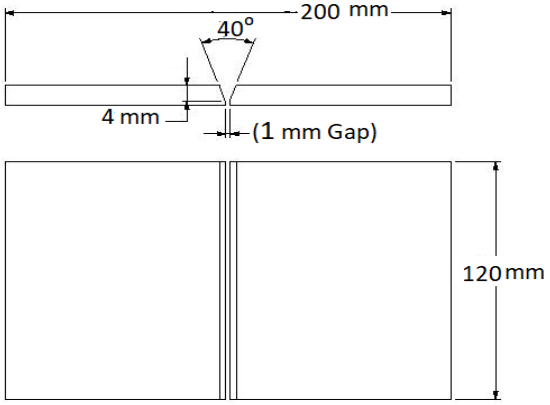

Figure 1. Dimensions and specifications of the tested piece

Table 1. Mechanical specifications of tested aluminum alloy pieces

Sample type	Yielding strength (0.2% offset) MPa	Ultimate strength MPa	elongation %	Elasticity modulus GPa	Hardness Brinell
H22 Al 5754	130	220-270	11	70.3	63

Table 2. The weight percent of both filler metals according to EN-573-3 standard

Wire mat.	≤ Si	≤ Fe	≤ Cu	≤ Mn	Mg	≤ Cr	≤ Zn	≤ Ti
ER-5754	0.4	0.4	0.1	0.5	2.6-3.6	0.3	0.2	0.15
ER-5356	0.25	0.4	0.1	0.2	4.5-5.5	0.2	0.1	0.2

The samples were numbered from 1 to 9 according to Table 4. The non-destructive tests (NDT) performed on the welded parts include visual, penetrating, and ultrasonic tests to determine the possible defects of the resulting weld. In addition, tensile strength and micro-hardness tests were performed to check the behavior of the created connection. Microstructures were examined by an optical microscope. Finally, all these tests were compared with the samples welded by the FSW method [20, 22, 23]. To perform the tensile test, samples were first prepared according to the ASTM E8-M standard.

As can be seen in Figure 2, the samples were cut into the desired shape and dimensions by a wire-cut machine. After that, it was subjected to a tensile strength test by the Shimadzu AG-25TA universal tensile testing machine. The results of the tensile test can provide important information about the modulus of elasticity, ultimate stress, fracture stress, and percentage of elongation of the samples before failure.

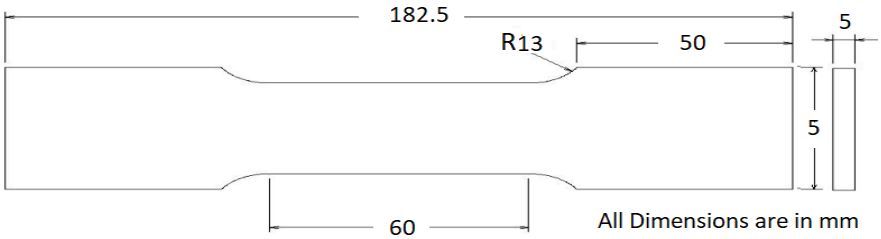

Figure 2. Making the samples by wire cut machine in a tensile strength test

Table 3. Taguchi method for selecting the TIG welding parameters

Welding parameters	Level 1	Level 2	Level 3
Argon flow (liters per minute)	15	17.5	20
Current intensity (A)	130	140	150
Speed (cm/ min)	8	10	12

Table 4. Taguchi method for TIG welding method along with 3 parameters and 3 levels for each parameter

No	Taguchi parameters arrangement			Argon flow (liters per minute)	Current (Amper)	Welding speed (cm/min)
1	1	1	1	15	130	8
2	1	2	2	15	140	10
3	1	3	3	15	150	12
4	2	1	3	17.5	130	12
5	2	2	1	17.5	140	8
6	2	3	2	17.5	150	10
7	3	1	2	20	130	10
8	3	2	3	20	140	12
9	3	3	1	20	150	8

Vickers hardness tester has been used to measure the hardness of the welded samples by FSW and TIG methods and compare it with the base metal. In this method, the welded samples were cut crosswise and then the samples were polished and etched. The hardness measuring device was set with a force of 50 newtons for 15 seconds. Then a hardness test was performed at intervals of 1 mm and the data of 15 points with the center of the weld axis were recorded in each sample [22]. To check the microstructure, the flat surface of the cut samples was primarily sanded with different sandpapers,

and then polishing was done on them. Then, the sample pieces were etched in solution with the chemical percentage specified in Table 5 for 10 seconds. To examine the samples in the welding area, imaging was done by optical and scanning electron microscopes (ESM). In this test, the microstructure and grain size of the alloys in the weld zone were determined.

Table 5. Chemical percentage of the solution

HCl	HNO_3	HF	Water
1.5 cc	2.5 cc	0.5 cc	95 cc

3. Data analysis

Initially, the raw samples were chemically analyzed before welding, the result of which is recorded in Table 6 based on the percentage of different elements. The tensile strength results of the preliminary part after chemical analysis are given in Table 7.

Table 6. The results of chemical analysis for raw pieces

Material	Si	Fe	Cu	Mn	Mg	Cr	Ni	Zn	Ti	V
AL5754	0.28	0.29	0.04	0.25	2.6	0.02	0.08	0.04	0.007	0.02

Table 7. The results of tensile strength for the primary piece after chemical analysis

Rolling direction	Ym (Mpa)	Y 0.2 (Mpa)	Elongation at fracture (%)	Hardness (HV)
longitudinal	210	126	37	58
Transverse	200	114	40	

The percentage of the elements of the materials obtained from the AA5754 material testing machine. The selected variables, including cooling gas flow rate, current intensity, and welding speed, were considered to achieve a weld with high strength and no defects in the form of the Taguchi table. The number of parts to be welded was 9 samples, which were subjected to tensile and hardness tests and microstructure examination after welding.

3.1 Visual inspection of welding

Visual test (VT) is the first step in weld inspection and examination of manufactured parts. If a part is found defective in VT, in more than 90% of cases, it is not necessary to apply other NDTs on it, because the imperfection size is big enough to see and generally parts will be rejected. But if the part has no problem in terms of VT, it may be necessary to test the part under other non-destructive processes for more certainty.

Figure 3. A and B show the top surface and the root of the weld appearance in the confirmed parts after the VT

In the VT, it was tried to examine the appearance of the weld and external defects such as the general appearance of the weld, the presence of oxide layers or corrosion products and cracks, the direction and position of cracks, surface porosity, unfilled holes, lack of penetration, the shape of the weld line and the possible orientation of the weld connection. Finally, the sources prone to mechanical weaknesses such as sharp grooves and misalignments should be checked in all parts. It is worth mentioning that out of 9 welded items, only 3 samples were confirmed by visual test, which includes samples of rows 3, 4, and 9 of Taguchi's Table 4. The reason for the non-confirmation of other samples was attributed to the insufficient root penetration of the weld. Figure 3 shows the appearance

of the welds made in the approved parts after the visual test. According to the figures, it can be seen that the appearance of the weld as well as the amount of penetration in the weld line in all 3 parts are acceptable and they have the necessary conditions to start the test. The figures in rows A and B show the top surface and root of the weld respectively. This is only an external inspection and the approval of the parts at this stage does not mean the final approval of the part and the approval of all welding conditions.

3.2 Penetrating liquid test

Liquid Penetrant Test (PT) is one of the most popular Nondestructive Examination (NDE) methods in the industry. It is economical, versatile, and requires minimal training when compared to other NDE methods. Liquid penetrant test checks for material flaws open to the surface by flowing a very thin liquid layer into the flaw and then drawing the liquid out with a chalk-like developer. The dye penetrant solvent removable method is the most popular because it is low-cost and very versatile. It typically comes in three aerosol cans, cleaner, penetrant, and developer. Figure 4 shows a test sample of penetrating liquid on the sample of row 3 of Table 4. This test can only show the surface defects of the weld, and defects such as lack of penetration, the presence of holes, and internal porosity of the weld, which are all related to the inside of the weld, should be discovered by other NDT processes. PT, which has a high relative speed, is usually used before tests such as ultrasonic test (UT) and radiographic test (RT). This test, which is performed according to the ASTM E165 standard, includes the steps of cleaning the welded area, impregnating the surface with penetrating liquid, dwell time of 20 minutes, cleaning the excess penetrating liquid from the surface, drying the surface, impregnating the surface with developing liquid, viewing the results and finally washing was done. After performing this test on the samples, no defects were observed on the upper surface of the formed weld.

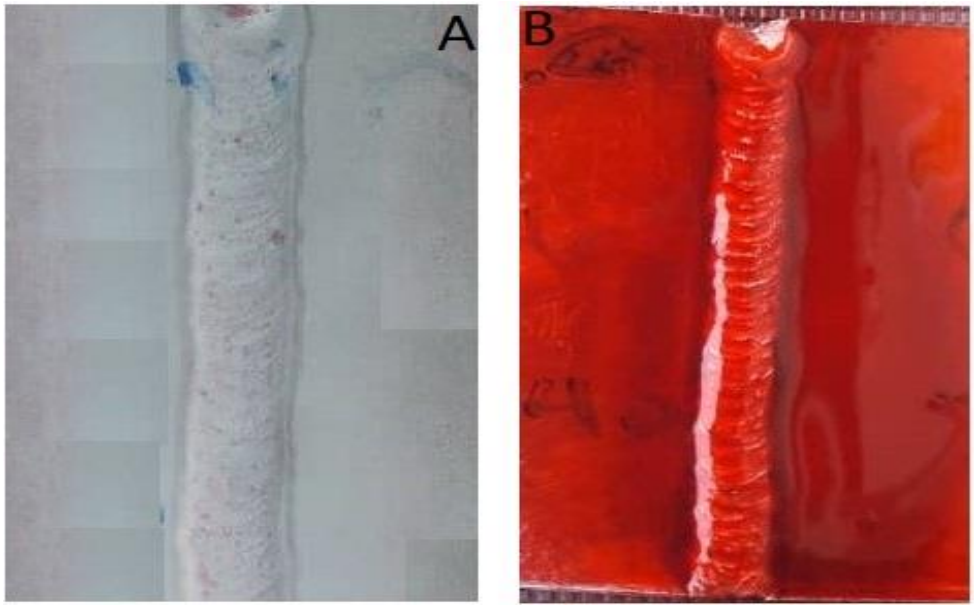

Figure 4. Testing the penetrative liquid in part 3, (A) After the PT and (B) after applying the penetrating liquid

3.3 Ultrasonic Test (UT)

Ultrasonic testing (UT) is a family of non-destructive testing techniques based on the propagation of ultrasonic waves in the object or material under the test. In most common UT applications, very short ultrasonic wave length pulses with frequencies ranging from 0.1-15 MHz and occasionally up to 50 MHz, are transmitted into materials to detect internal flaws or to characterize materials. If the part surface is smooth, UT can detect almost all surface and subsurface defects. In ultrasonic testing, a transducer connected to the device is used to send sound waves into the material, and it often requires the use of a coupling (such as oil or water) to connect the transducer and the object, which increases the accuracy of the results. Therefore, to be sure of the absence of defects, as well as to check and detect the size of defects, UT was used in this research. In UT, lower frequencies have more penetrating power but less sensitivity. While higher frequencies less penetrate, they can detect smaller defect signs. Also, sensitivity, resolving power, dead zone, and near-field effect are the most important characteristics of an ultrasonic probe. In this test, the USM35 device was used, whose settings are based on the sensor that receives and transmits sound waves of 2 MHz, with a normal angle and sound speed of 6320, and longitudinal waves. It should be noted that in this test, no defects were observed in the three approved samples of the tested parts.

3.4 Tensile test

After preparation, the tensile test of samples 3, 4, and 9 was performed with a force of 5 tons and a speed of 2 mm/min in three stages. The output results of this test include information such as yield, ultimate and fracture stresses, and finally the percentage of elongation. These tests were performed only on the samples approved in previous inspections (VT, PT, and UT) and are shown in the diagram of Figures 5 to 7.

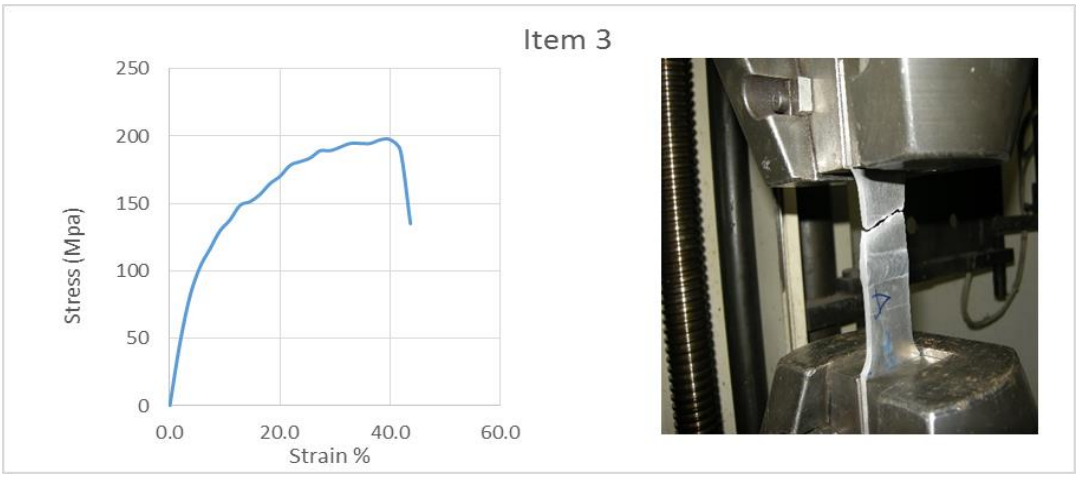

Figure 5. The strength diagram for part No. 3

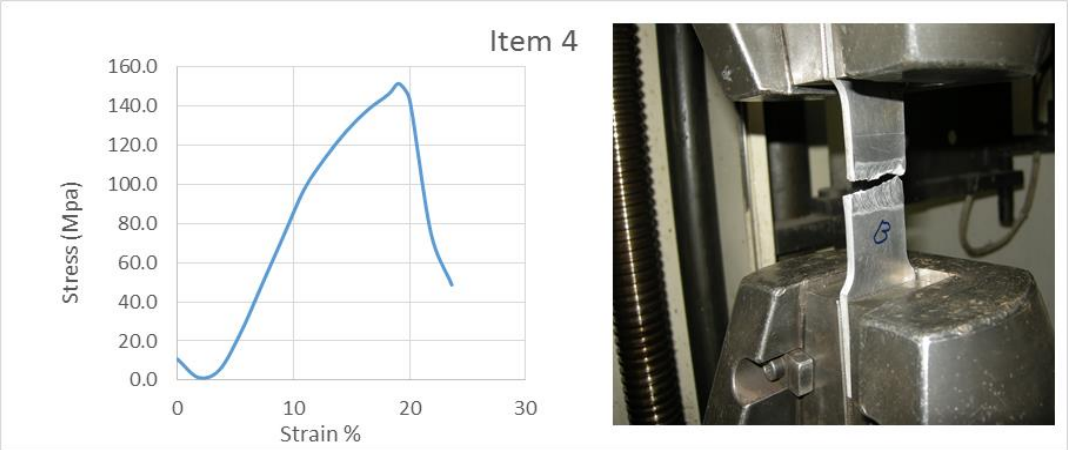

Figure 6. The strength diagram for part No. 4

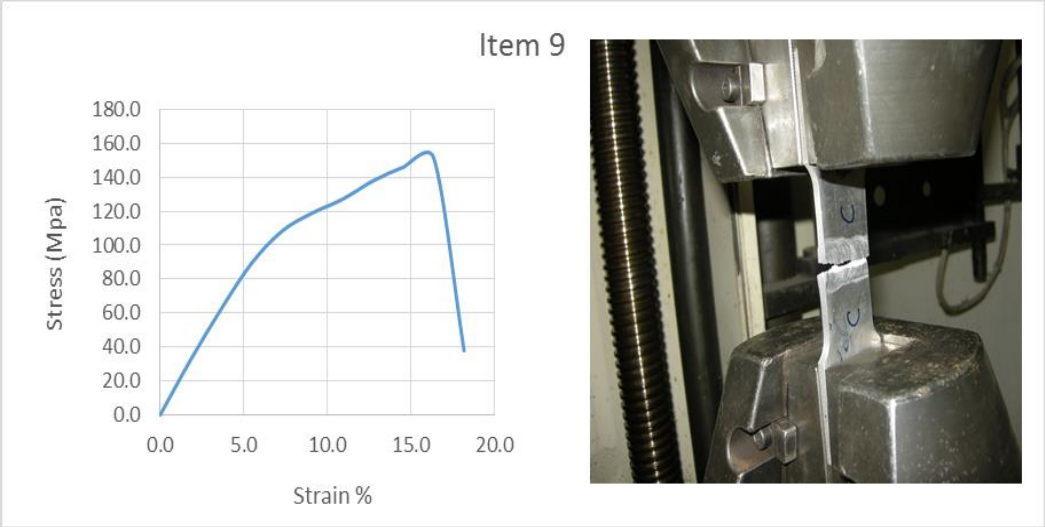

Figure 7. The strength diagram for part No. 9

From these graphs, it can be seen that sample number 3 has better mechanical properties compared to other parts (Table 8), which indicates proper welding with expected input parameters. From this, we can conclude that by choosing the optimal parameters for welding AL5754-H22 alloy, we can witness the maximum results of this process, which increases efficiency and reduces weight in structures of various industries such as automobile, shipbuilding, and aircraft.

Weld joint efficiency refers to the capacity of interconnected components in a system to function optimally while minimizing energy losses and maximizing mechanical advantage. Achieving efficient joints is crucial in ensuring the overall stability, performance, and longevity of these systems. As can be seen in Figures 6 and 7, the failure of row 4 and 9 samples occurred in the welding area, which is considered a weakness in welding, and the row 3 sample has higher strength and efficiency than the previous two samples. Therefore, it can be concluded that the best welding conditions for welding aluminum alloy 5754 are the conditions of the third-row sample given in Table 8. So, it was necessary to compare the third row with the FSW method [21-22].

Table 8. Parts of rows 3, 4, and 9 of Taguchi's table

Test item	Tensile Strength, Yield [0.2% offset] (MPa)	Tensile Strength, Ultimate (MPa)	Elongation at Break (%)	Joint efficiency (%)
3	93	195	38	92.8
4	95	152	13	76
9	87	151	13.30	75.5

3.5 Comparing the tensile test diagrams in FSW and GTAW modes

It is necessary to compare the graphs of these two methods with each other for a better understanding of FSW and TIG (GTAW). As seen in Figure 8, this comparison was between sample 3 as the highest efficiency in Taguchi's table, as well as FSW-F and FSW-A. By comparing the graphs, it was observed that the welding efficiency in TIG mode can be higher than the other two FSW methods [24-25].

3.6 Microhardness measurement test

As shown in Table 7, the hardness of the initial parts was measured as 58 Vickers. After TIG welding, the distribution of hardness in the weld profile was determined by measuring at fifteen points centered on the weld axis and at an interval distance of 1 mm from each other (Figure 9). The graph of Figure 9 shows that the distribution of the hardness level in the weld cross-section is continuously increased from the base metal and reaches its maximum in the center of the weld. This smooth variation in hardness indicates the lack of stress concentration in the HAZ after welding. Also, the maximum hardness in the weld center is higher due to the presence of magnesium element as a result of using ER5356 filler. This filler has about 2% more magnesium than the base metal, so it has been able to overcome its evaporation rate during welding and provide the necessary and sufficient strength in this zone.

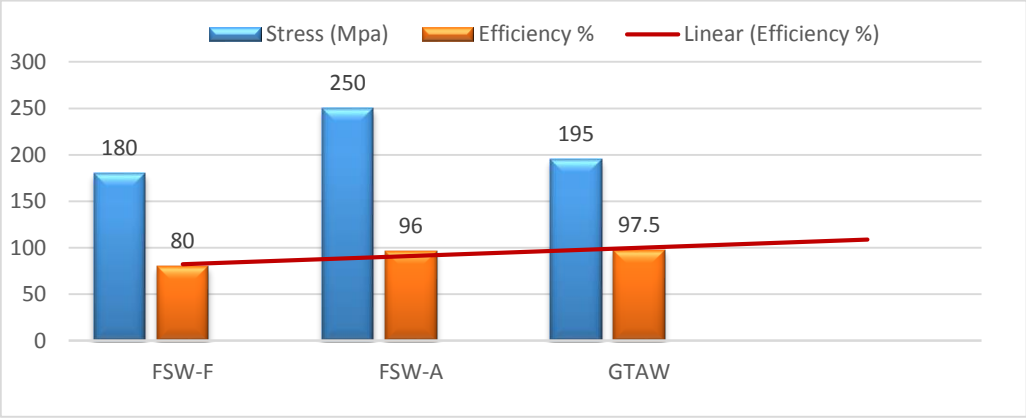

Figure 8. Graphical comparison of tensile test in FSW and TIG welding modes

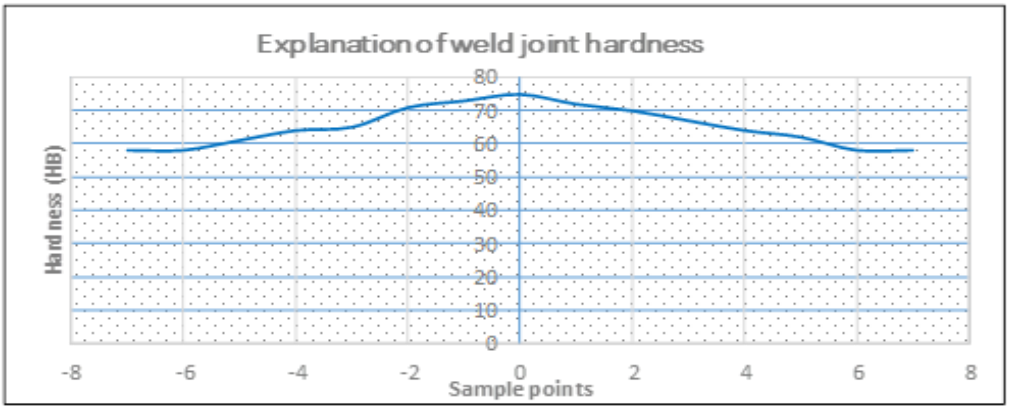

Figure 9. Hardness distribution diagram in weld profile

Since hardness and strength have a direct relationship, it can be concluded that the strength of the weld zone is higher than that of the base metal. This caused the fracture of the piece in the tensile test to happen outside of the weld zone and the heat-affected zone. Since the hardness of the part at a distance of 7 mm from the welding axis has reached the hardness of the base metal, it can be concluded that the amount of heat input of welding in sample 3 of Taguchi's table is appropriate. It should be accepted that the fracture of the metal in an area about 25 mm from the center of the weld and at an angle of 45 degrees can validate this claim.

3.7 Chemical composition of the weld zone

To determine the percentage of weight elements and estimate the strength of the weld zone, it was necessary to analyze the weld zone. As previously mentioned, and according to Table 9, the filler used in this research was selected as AA5356, which differs only in its magnesium percentage from the base metal. In the following, the effect of magnesium content in 5xxx group aluminum alloys will be discussed. The percentage of magnesium in commercial alloys ranges from 0.5 to 12-13 mg.

Table 9. The element's weight percent in the weld zone

%Mat.	Si	Fe	Cu	Mn	Mg	Cr	Ni	Zn	Ti	V	Rem.
Weld Zone	0.18	0.36	0.03	0.2	3.9	0.06	0.006	0.02	0.06	0.02	Al

Low magnesium alloys have the best formability and high magnesium alloys have high strength. It is common to make these alloys from higher grades of aluminum (99.7%) to obtain maximum resistance to corrosion and reflectivity. In general, the higher the amount of magnesium, the higher will be the strength of the metal. During the welding of work-hardened metals such as aluminum sheets with H characteristics, due to the high welding temperature, the strength of the HAZ is weak, and it is necessary to choose the right filler that can improve the strength of the welding zone. Considering that the piece of sample 3 is torn from the base material in the tensile test. Therefore, it can be considered the effect of the higher amount of magnesium in the welding zone as a result. One of the biggest advantages of fusion welding is the ability to choose welding fillers for welding ferrous and non-ferrous metals, especially 5000 group aluminum alloys, which is considered to create a high-strength weld by the TIG method. However, there are many limitations in methods such as FSW welding to increase the strength of the welding zone.

3.8 Examination of the microstructure

To check the microstructure and distribution of grains in the cross-section of the weld, in the first step, it was necessary to polish and etch the sample and then keep it in the Polar solution with specified percentages for 10 seconds. The results can be seen in Figure 10 (A to D). It should be noted that these images are prepared with restrictions that are mostly related to the materials of the sample. These limitations are in the etched section and an attempt has been made to provide clear images of the piece.

3.9 Metallographic analysis

From Figure 10, it can be seen that the welding is proper in the HAZ and the amount of heat affected by the welding process has not resulted in damage to the part in this zone.

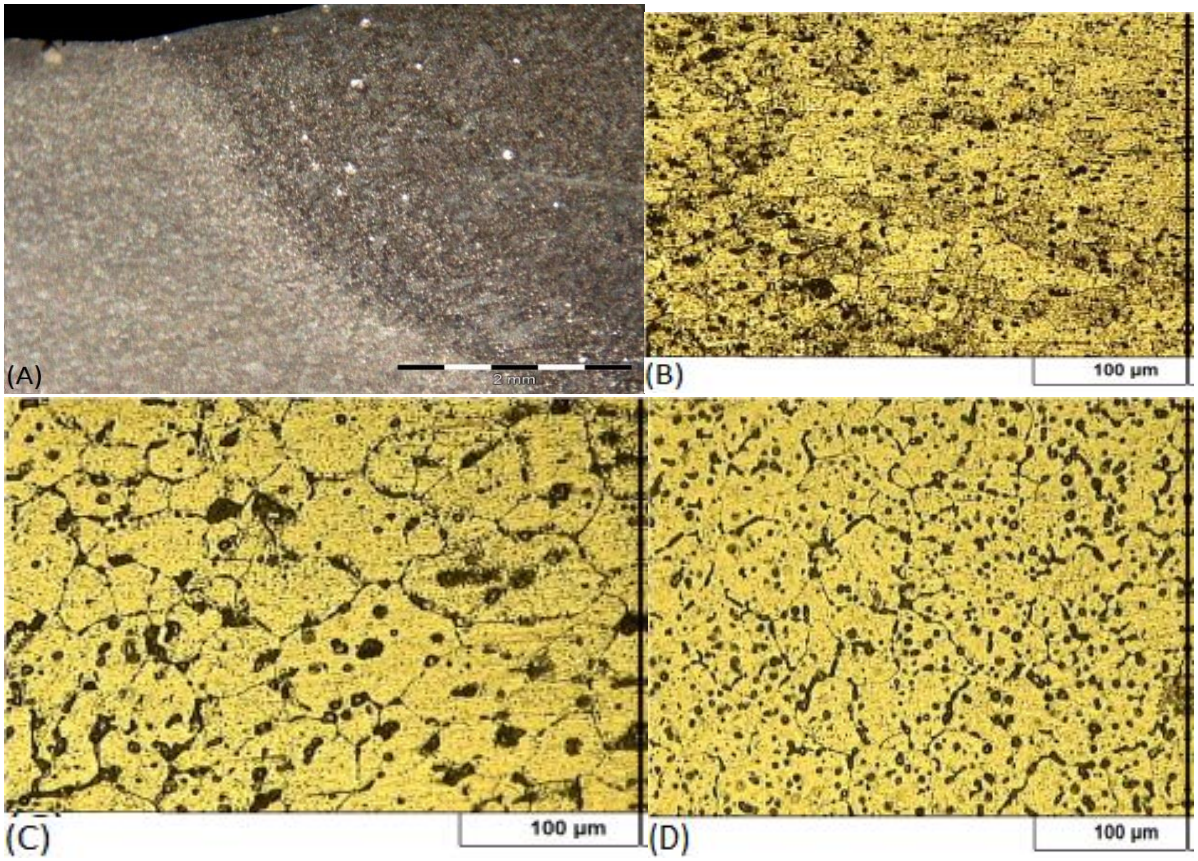

Figure 10. Microstructure of (A) Weld zone and Heat-affect zone: (B) Base metal, (C) HAZ, and (D) Weld area

In the images related to the base metal, the HAZ, and the welding zone, it can be seen that all three zones have a fine-grained structure, including the alpha solid solution phase, in which fine magnesium particles are distributed. According to the results of the metallographic test as well as the metallographic images of all three zones and their comparison, it can be seen that the size of the grains in the HAZ and the welding zone is the same and equal to 30 microns, that is smaller than the size of the grains of the base material, which is measured as 44 microns. This amount of size difference in the three regions causes a stress concentration to occur between the base metal and the HAZ due to the microstructural change which can be seen by examining the tensile test and the rupture region of

the sample. It can be seen that this difference in the grain size and the resulting stress concentration did not cause the sample to break from this region.

3.10 Comparison of tensile strength

In this research, FSW and TIG welding methods were first introduced. Next, the welding of the AA5754-H22 aluminum workpiece was investigated by the TIG method, and the necessary parameters were obtained to create a suitable and desirable weld. In this part, the final parts of this method will be compared with the FSW method and with almost the same alloy and physical characteristics. For this purpose, FSW-F welding characteristics and also FSW-A welding will be used [22, 23]. It should be noted that due to the difference in the mechanical characteristics of the materials, it was decided to calculate the efficiency of the welding methods. Finally, by presenting a table, the appropriate method was chosen. Table 10, shows the strength of the base metal along with the final strength of different welding methods. In this table, it is clear that the efficiency of the TIG method is higher than other methods.

Table 10. The strength of base metal along with the ultimate strength of different welding methods

Test item	Yield (0.2% offset) (MPa)	Ultimate Strength (MPa)	Ultimate Strength, Base metal (MPa)	Elongation at Break (%)	Joint efficiency (%)
TIG	93	195	210	38	92.8
FSW-F [22]	95	180	225	37.5	80
FSW-A [23]	-	250	260	-	96

3.11 Hardness profile comparison

Figure 11, shows the hardness profiles of all three processes. It seems that the distribution of hardness in the weld zone, HAZ, and base metal in the FSW-A diagram is non-uniform and has a fluctuation of about 10 units in a relatively large range. But in the FSW-F chart, there are more fluctuations, the amount of which is about 5 units in a small range of 3 mm.

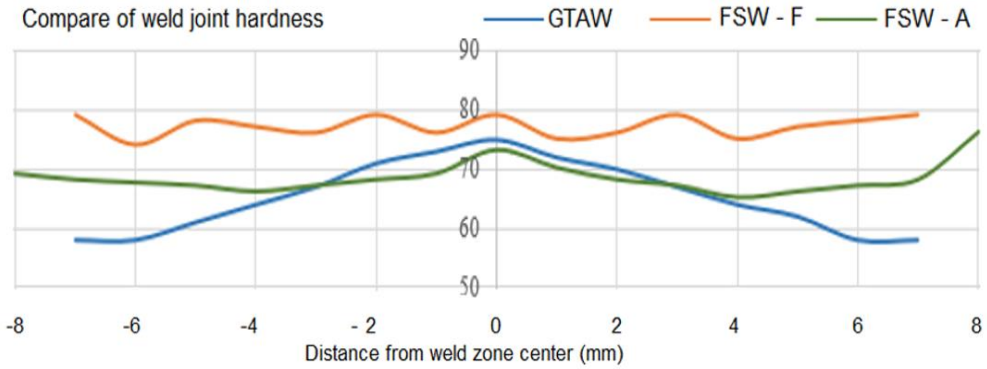

Figure 11. The hardness profile diagram for FSW-F, FSW-A and TIG processes [18]

There is not much fluctuation in the TIG graph and only the hardness value has decreased uniformly from the maximum value to its minimum value with a difference of 17 units. It is impossible to obtain a uniform hardness profile in the weld zone and its surroundings in TIG welding. The absence of

fluctuation of hardness can increase the concentration of stress in the HAZ, and increase the strength of the metal against fatigue and tensile stresses, which can be seen in the TIG welding method.

3.12 The microstructure comparison

In this part, metallographic images related to TIG and FSW methods are discussed. Figure 12 shows that the particles of intermetallic magnesium element are scattered in the α-phase aluminum substrate in both welding methods. Also, the size of base metal grains in the FSW welding method is between 3.5 and 4.5 micrometers, and in the TIG method is about 44 micrometers, which generally indicates the base metal with different grain sizes for both methods.

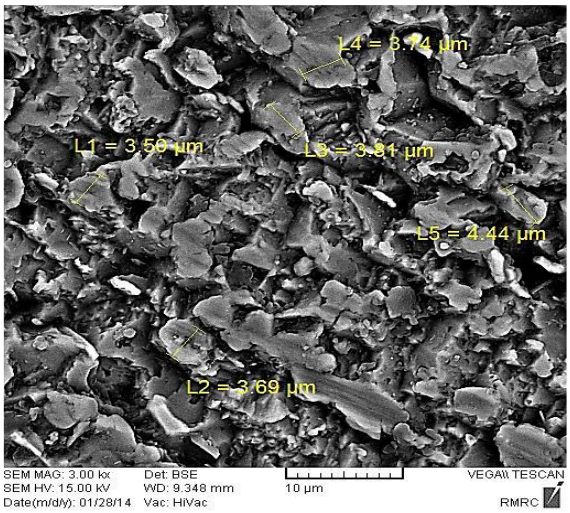

Figure 12. The grain size of base metal for FSW [19]

Figure 13, shows the microscopic image of the FSW method. The width of the HAZ varies from a minimum of 30 microns to a maximum of 120 microns, while the width of the HAZ in the TIG method, which is specified in Figure 10A, is measured at the same level of 3 micrometers. This shows that the FSW method has been effective in reducing the HAZ and the TIG method in making this area uniform after welding. Figure 14, which is related to the FSW, the size of the grains in the welding area has been measured in the range of 4.9 to 6.5 microns. Meanwhile, in the TIG method, the grain size of the weld zone is 30 micrometers (Figure 10D). It should be noted that the grain size has become larger after FSW, but it is observed that it has become smaller after TIG welding. The small size of the grains and the small difference in their size in the triple zone compared to each other make it possible to provide better mechanical properties.

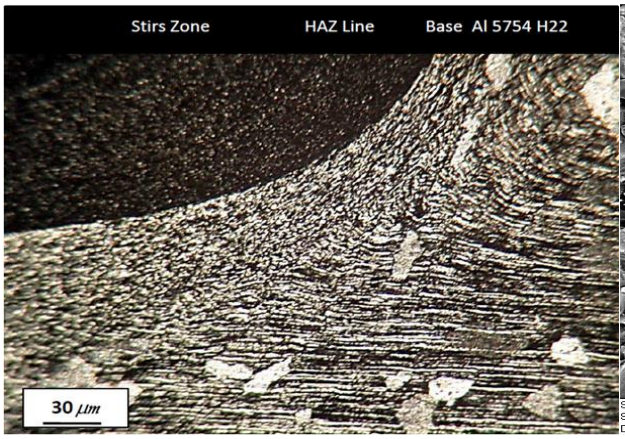

Figure 13. The microscopic picture of HAZ for FSW [23].

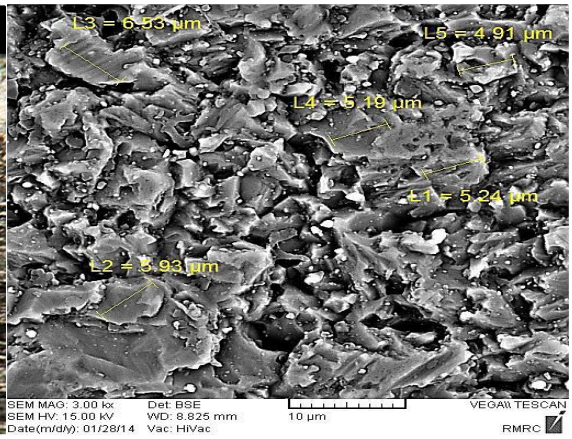

Fig. 14- The grain size of the welding zone for FSW [23].

In terms of the metal properties, there are other things to consider when evaluating those of the HAZ itself. Due to the variations in temperature across the HAZ, the individual portions will have differing properties as they see different temperatures for different amounts of time. This fact, and its importance or otherwise, is beyond the scope of this article but may be covered in a sister article at a future date.

4. Conclusion

According to the tests and analyses carried out on the welded samples with both TIG and FSW methods, it was determined that:

- The TIG method has higher tensile strength efficiency for samples 3, 4, and 9. The tensile strength values are 195, 152, and 151 MPa, respectively, and in addition, it has better slope uniformity in the hardness section.
- In the microstructure section, it can be stated that in the FSW method, due to the finer grain size of the base metal (44 microns), the joining has a better microstructure (30 microns) than the TIG method. Finer grains make some mechanical properties such as toughness, fatigue strength, and flexibility higher in the FSW method.
- In any welding method, the hardness and strength of the welding area are lost but in the TIG method by changing the welding filler material it can be compensated, so it can be considered that the TIG process is preferred in terms of tensile strength and hardness compared to friction welding.
- According to the results of the metallographic test of all three areas (base metal, heat-affected area, and welding area), it can be seen that the grain size in the HAZ and the welding area is the same equal to 30 microns. This is smaller than the base metal, which is measured at 44 microns. This amount of size difference in these zones caused some stress concentration to occur between the base metal and the HAZ due to the microstructure change. Examining the tensile test and the rupture area of the sample showed that this difference in the size of the grains and the resulting stress concentration did not cause any sample break in this area.

5. References

[1] Manjhi, S.K., Das, A. and Prasad, S.B. 2020. Review on joining of aluminum alloy by solid-state welding technique. Materials Today: Proceedings. 26:1255-1261. doi: 10.1016/j.matpr.2020.02.251.

[2] El-Sayed, M.M., Shash, A.Y., Abd-Rabou, M. and ElSherbiny, M.G. 2021. Welding and processing of metallic materials by using friction stir technique: A review. Journal of Advanced Joining Processes. 3:100059. doi.org/10.1016/j.jajp.2021.100059.

[3] Mishra, R.S. and Ma, Z.Y., 2005. Friction stir welding and processing. Materials science and engineering: R: reports, 50(1-2), pp.1-78. doi:10.1016/j.mser.2005.07.001.

[4] Ahmed, M.M., El-Sayed Seleman, M.M., Fydrych, D. and Çam, G. 2023. Friction stir welding of aluminum in the aerospace industry: the current progress and state-of-the-art review. Materials. 16(8):2971. doi:10.3390/ma16082971.

[5] Masoumi Khalilabad, M., Zedan, Y., Texier, D., Jahazi, M. and Bocher, P. 2022. Effect of heat treatments on microstructural and mechanical characteristics of dissimilar friction stir welded 2198/2024 aluminum alloys. Journal of Adhesion Science and Technology. 36(3):221-239. doi:10.1080/01694243.

[6] Niazi, M., Afsari, A., Behgozin, A. and Nazemosadat, M.R. 2023. Multi-objective optimization of kinematic tool parameters in FSW of Al-7075 and Al-6061 alloys by RSM. Journal of Welding Science and Technology of Iran. 9(1):17-29.

[7] Kumar, K.V. and Balasubramanian, M. 2020. Analyzing the effect of FSW process parameter on mechanical properties for a dissimilar aluminum AA6061 and magnesium AZ31B alloy. Materials Today: Proceedings, 22, pp.2883-2889. doi:10.1016/j.matpr.2020.03.421.

[8] Woźny, P. and Błachnio, J., 2018. Managing the influence of microstructure defects on the strength of EN AW 5754 aluminium alloy welded joints executed with the TIG method. In MATEC Web of Conferences. 182:02025. EDP Sciences. doi.org/10.1051/matecconf /201718202025.

[9] Park, S.K., Hong, S.T., Park, J.H., Park, K.Y., Kwon, Y.J. and Son, H.J. 2010. Effect of material locations on properties of friction stir welding joints of dissimilar aluminium alloys. Science and Technology of Welding and Joining, 15(4):331-336.doi:10.1179/136217110X12714217309696.

[10] Munoz, A.C., Rückert, G., Huneau, B., Sauvage, X. and Marya, S. 2008. Comparison of TIG welded and friction stir welded Al–4.5 Mg–0.26 Sc alloy. Journal of materials processing technology. 197(1-3):337-343. doi:10.1016/j.jmatprotec.2007.06.035.

[11] Shanavas, S. and Dhas, J.E.R. 2017. Weldability of AA 5052 H32 aluminium alloy by TIG welding and FSW process–a comparative study. In IOP Conference Series: Materials Science and Engineering. 247(1):012016. IOP Publishing. doi:10.1088/1757-899X/247/1/012016.

[12] Liyakat, N.A. and Veeman, D. 2022. Improvement of mechanical and microstructural properties of AA 5052-H32 TIG weldment using friction stir processing approach. Journal of Materials Research and Technology. 19:332-344. doi:10.1016/j.jmrt.2022.05.015.

[13] Habba, M.I.A., Alsaleh, N.A., Badran, T.E., El-Sayed Seleman, M.M., Ataya, S., El-Nikhaily, A.E., Abdul-Latif, A. and Ahmed, M.M.Z. 2023. Comparative study of FSW, MIG, and TIG welding of AA5083-H111 based on the evaluation of welded joints and economic sspect. Materials. 16:5124. doi: 10.3390/ma16145124.

[14] Grover, H.S., Chawla, V. and Brar, G.S. 2017. Comparing mechanical and corrosion behaviour of TIG & FSW weldments of AA5083-H321. Indian Journal of Science and Technology. 10(45):1-8. doi:10.17485/ijst/2017/v10i45/113537.

[15] Barakat, A.A., Darras, B.M., Nazzal, M.A. and Ahmed, A.A. 2022. A comprehensive technical review of the friction stir welding of metal-to-polymer hybrid structures. Polymers. 15(1):220. doi.org/10.3390/polym15010220.

[16] Sharma, A. and Dwivedi, V.K. 2020. Comparison of micro structural and mechanical properties of aluminium alloy AA6062 on FSW and TIGW processes. Materials Today: Proceedings. 25:903-907. doi:10.1016/j.matpr.2019.12.429.

[17] Isa, M.S.M., Moghadasi, K., Ariffin, M.A., Raja, S., bin Muhamad, M.R., Yusof, F., Jamaludin, M.F., bin Yusoff, N. and bin Ab Karim, M.S. 2021. Recent research progress in friction stir welding of aluminium and copper dissimilar joint: a review. Journal of Materials Research and Technology. 15:2735-2780. doi:10.1016/j.jmrt.2021.09.037.

[18] Abbasi, M., Givi, M. and Bagheri, B. 2020. New method to enhance the mechanical characteristics of Al-5052 alloy weldment produced by tungsten inert gas. Proceedings of the Institution of Mechanical Engineers, Part B: Journal of Engineering Manufacture. 0954405420929777. doi:10.1177/0954405420929777.

[19] Yelamasetti, B., Sridevi, M., Sree, N.S., Geetha, N.K., Bridjesh, P., Shelare, S.D. and Prakash, C. 2024. Comparative studies on Mechanical properties and Microstructural changes of AA5052 and AA6082 dissimilar weldments developed by TIG, MIG, and FSW techniques. Journal of Materials Engineering and Performance. 1-14. doi: 10.1007/s11665-024-09867-9.

[20] Afsari, A., Heidari, S. and Jafari, J. 2020. Evaluation of optimal conditions, microstructure, and mechanical properties of aluminum to copper joints welded by FSW. Journal of Modern Processes in Manufacturing and Production, 9(4):61-81. dor: 20.1001.1.27170314.2020.9.4.6.4.

[21] Blachnio, J., Kulaszka, A., Chalimoniuk, M. and Wozny, P. 2016. Exemplification of tomographic method to evaluate the quality of welded joints made from EN 5754-H22 alloy. Research Works of Air Force Institute of Technology. 39(1):65-78. doi:10.1515/afit-2016-0018.

[22] Durmuş, H. and Çömez, N. 2017. Mechanical properties of AA5754 sheets welded by cold metal transfer method. Technological Applied Sciences, 12(4):170-177. doi:10.12739/NWSA.2017.12.4.2A0124.

[23] Rajeshkumar, R., Niranjani, V.L., Devakumaran, K. and Banerjee, K. 2021. Fusion boundary microstructure evolution and mechanical properties of cold metal transfer welded dissimilar A5754 and A5083 joint. Materials Letters. 284:128877. doi:10.1016/j.matlet.2020.128877.

[24] Rabie Zadeh, A. and Afsari, A. 2016. Production of Dispersed Ceramic Nano-Particles in Al Alloy Using Friction Stir Processing. Journal of Modern Processes in Manufacturing and Production. 5(3):41-57.

[25] Eessa, A., Yousif, M. and El-Nikhaily, A. 2015. Effect of tool pin eccentricity on mechanical properties and microstructure of friction stir welded 5754 aluminum alloy. Port-Said Engineering Research Journal. 19(1):108-113. doi: 10.21608/pserj.2015.36789.